

# Excitonic recombinations in hBN: from bulk to exfoliated layers

A. Pierret,<sup>1,2</sup> J. Loayza,<sup>1,3</sup> B. Berini,<sup>3</sup> A. Betz,<sup>4,\*</sup> B. Plaçais,<sup>4</sup> F. Ducastelle,<sup>1</sup> J. Barjon,<sup>3</sup> and A. Loiseau<sup>1</sup>

<sup>1</sup>*Laboratoire d'Etude des Microstructures, ONERA-CNRS, BP 72, 92322 Châtillon Cedex, France*

<sup>2</sup>*CEA-CNRS group "Nanophysique et Semiconducteurs",*

*Institut Néel/CNRS-Univ. J. Fourier and CEA Grenoble, INAC,*

*SP2M, 17 rue des Martyrs, 38054 Grenoble Cedex 9, France*

<sup>3</sup>*Groupe d'Etude de la Matière Condensée, University of Versailles St-Quentin and CNRS,*

*45 avenue des Etats-Unis, 78000 Versailles, France*

<sup>4</sup>*Laboratoire Pierre Aigrain, ENS-CNRS UMR 8551,*

*Universités P. et M. Curie and Paris-Diderot, 24, rue Lhomond, 75231 Paris Cedex 05, France*

Hexagonal boron nitride (h-BN) and graphite are structurally similar but with very different properties. Their combination in graphene-based devices meets now a huge research focus, and it becomes particularly important to evaluate the role played by crystalline defects in them. In this work, the cathodoluminescence (CL) properties of hexagonal boron nitride crystallites are reported and compared to those of nanosheets mechanically exfoliated from them. First the link between the presence of structural defects and the recombination intensity of bound-excitons, the so-called D band, is confirmed. Low defective h-BN regions are further evidenced by CL spectral mapping (hyperspectral imaging), allowing us to observe new features in the near-band-edge region, tentatively attributed to phonon replica of exciton recombinations. Second the h-BN thickness was reduced down to six atomic layers, using mechanical exfoliation, as evidenced by atomic force microscopy. Even at these low thicknesses, the luminescence remains intense and exciton recombination energies are not strongly modified with respect to the bulk, as expected from theoretical calculations indicating extremely compact excitons in h-BN.

## I. INTRODUCTION

Hexagonal boron nitride (h-BN) has the same honeycomb lattice as graphite with two atoms per unit cell and similar lattice parameters. Due to this similarity, boron nitride materials attract a growing interest in line with the development of low-dimensional carbon-related materials. As for carbon, BN materials can be synthesized either as nanotubes (1D form)<sup>1,2</sup> or as mono/multi layers (2D form).<sup>3,4</sup> In the following we focus on this latter form. 2D layers of carbon, namely graphene sheets, display extraordinary electronic properties which open unanticipated routes for a new generation of electronic devices. However, electronic performances, initially observed in suspended graphene, can be dramatically degraded by detrimental effects of substrate disorder and adsorbents. Facing this problem, h-BN layers (also called white graphene) are of particular interest as support or capping layers of graphene. They indeed combine several properties: they are insulating (h-BN is a large gap semiconductor due to the polar BN bond),<sup>5–7</sup> they display an especially compatible layered  $sp^2$  structure with that of graphene, which ensures no dangling bond or surface charge trapping and a low roughness of easily cleaved planes. As a matter of fact, graphene transferred on BN layers displays an electron mobility at room temperature of  $60\,000\,cm^2/Vs$ , which is the highest reported value for a supported graphene and very close to that of suspended graphene.<sup>8–11</sup> Beyond, the high compatibility between graphene and BN sheets in terms of their lattice may lead to the emergence of a new class of BN/graphene/BN heterostructures for in plane or vertical transport stacking. In the first case, BN can act as a support or di-

electric layer that preserves the electronic properties of graphene,<sup>8</sup> while in the second case, graphene layers act as tunable metallic electrodes for the BN quasi-ideal tunnel barrier.<sup>12</sup> These promising perspectives have been yet demonstrated from pioneering experiments done using mechanically exfoliated sheets from both graphite and h-BN single crystals. In the future, h-BN and graphene based devices and heterostructures would most probably use CVD made polycrystalline films and sheets. Their performances would only be achieved via an accurate control of the defects in both graphene and BN layers and of the layers engineering. While the electronic properties of graphene are well-described theoretically and investigated experimentally, this is not the case of BN layers and even of h-BN. This is due to both the scarcity of high quality materials and to the nature of their electronic properties dictated by the large gap. It is thus a basic issue to understand the spectroscopic properties of atomically thin h-BN layers and their intrinsic defects, which is the focus of this Letter.

In contrast to graphene, usual spectroscopic characterization techniques such as Raman are handleless or provide a poor information when used for h-BN. Absorption and luminescence spectroscopies have been shown to be the most direct approach to investigate the electronic properties of BN materials, due to their large gap. To this aim, dedicated cathodo- and photo-luminescence experiments have been recently developed and applied to BN powders and single crystals.<sup>6,13–15</sup> Both theoretical calculations<sup>16–19</sup> and most recent excitation photoluminescence experiments on single crystals<sup>6</sup> converge to establish the bandgap of h-BN near 6.4 eV. Furthermore, it is now commonly accepted that h-BN optical properties

are dominated by huge excitonic effects. The near-band-edge luminescence spectrum is composed of two series of lines. Referring to measurements done on single crystals in Ref. [14], they are defined as the S and D bands. The four higher energy lines, labeled S1 to S4, located between 5.7 and 5.9 eV, are attributed to the exciton, whereas the lower energy ones, labeled D1 to D4, between 5.4 and 5.65 eV, are assigned to excitons bound to structural defects.<sup>13,14</sup> The excitons in h-BN are more of Frenkel-type than of Wannier-type (as in others usual semiconductors, such as AlN with a 6.1 eV gap). Ab-initio calculations indeed predict that the spatial extension of the exciton wavefunction is of the order of one h-BN atomic layer.<sup>16-19</sup> Moreover the experimental Stokes-shift of 250 meV observed for the S4-band suggests its self-trapping,<sup>6,14</sup> consistent with the very localized view of the Frenkel exciton.

To complete this view, the effect of a reduction in the h-BN thickness down to the atomic level has to be analyzed. Up to now, only scarce studies deal with the optical properties of nanometer-thick BN layers. Some of these report an optical absorption edge between 5.6 and 6.1 eV at room temperature,<sup>3,4,20-26</sup> i.e. in the same range than in bulk h-BN. Only two studies report near-band edge recombination luminescence, with no correlation to the BN layer thickness under investigation.<sup>21,27</sup>

In this Letter we present the first study of the luminescence properties of single BN nanosheets, with well-known thickness, by combining atomic force microscopy (AFM) and cathodoluminescence (CL) measurements. Large CVD made BN layers being not yet easily available, BN nanosheets were prepared by mechanical exfoliation of small h-BN crystallites of a polycrystalline powder. This material offers the advantage to give access in the same time to the intrinsic optical response of the crystallite as well as the effect of grain boundaries and the crystallite thickness on this response. An advanced characterization of the starting bulk material is first presented and its near-band-edge recombinations observed by CL are discussed with respect to that of single crystal. Then the luminescence of the exfoliated BN sheets is presented and discussed as a function of their thickness.

## II. EXPERIMENTAL

### A. Samples and exfoliation process

The bulk material exfoliated in this work is the high purity TRÈS BN<sup>©</sup> St-Gobain commercial power PUHP1108, used in cosmetic applications. The h-BN crystallites are already shaped as flakes with large (00.1) surfaces of typically 10  $\mu\text{m}$  diameter, which is particularly convenient for the exfoliation process. Their thickness is about 100 nm. One of these crystallites is shown in the scanning electron microscope (SEM) image of Figure 1a. This powder was synthesized at high temperature from boric acid and a nitrogen source. Our measurements

on this powder are compared with the ones obtained from a single crystal of the best available quality, synthesized by a high-pressure high-temperature (HPHT) crystal process<sup>28</sup> and provided by Taniguchi et al. This reference sample is called hereafter the HPHT sample.

Exfoliation of few-layer h-BN was carried out by mechanical peeling following the same method used for graphene.<sup>29</sup> The powder is applied to an adhesive tape, whose repeated folding and peeling apart separates the layers. These thin layers are then transferred on a Si wafer covered with 90 nm of  $\text{SiO}_2$ , which is the optimal thickness for imaging BN flakes with the maximum contrast.<sup>30</sup> Prior to the h-BN deposition, Cr/Au localization marks were formed on the wafer by means of UV-lithography using AZ5214E photo-resist and Joule evaporation.<sup>31</sup> The marks facilitate the localization of the flakes for the different measurements to be achieved of the same flake. Still prior to transferring the layers, the wafer is chemically cleaned with acetone and isopropanol, followed by several minutes exposure to a strong  $\text{O}_2$  plasma (60 W,  $P \leq 12 \text{ nbar}$ ). This last step eliminates most contaminants but also renders the  $\text{SiO}_2$  surface hydrophilic,<sup>32</sup> which has the drawback of facilitating the inclusion of a thin water layer between the flakes and the substrate.<sup>32,33</sup> As we shall see later, this complicates the layer thickness measurement done by atomic force microscopy (AFM).

### B. Cathodoluminescence procedure

The cathodoluminescence of the h-BN samples was analyzed at low temperature in the (i) spectroscopic (ii) imaging and (iii) spectral mapping modes, using an optical system (Horiba Jobin Yvon SA) installed on a high resolution JEOL7001F field-emission scanning electron microscope. The samples are mounted on a GATAN cryostat SEM-stage and cooled down to  $\approx 20 \text{ K}$  with a continuous flow of liquid helium. They are excited by electrons accelerated at 5 kV with a beam current as low as 0.17 nA. The CL emission is collected by a parabolic mirror and focused with mirror optics on the entrance slit of a 55 cm-focal length monochromator. The all-mirror optics combined with a suited choice of UV detectors and gratings ensures a high spectral sensitivity down to 190 nm. A silicon charge-coupled-display (CCD) camera is used to record spectra in mode (i) and as well for the spectral mapping mode (iii). In mode (iii), also referred as the hyperspectral imaging acquisition mode, the focused electron beam is scanned step-by-step with the *HJY CL Link* drive unit (co-developed and tested at GEMaC) and synchronized with the CCD camera to record one spectrum for each point. The spectrometer is also equipped with a UV photomultiplier on the lateral side exit for fast monochromatic CL imaging (i.e. image of the luminescence at a given wavelength) in mode (ii). For all spectra reported in this paper, it was checked that the linewidths are not limited by the spectral reso-

lution of the apparatus (0.02 nm in the best conditions). In the case of h-BN exfoliated layers, CL was only performed in mode (i) and using a fast e-beam scanning of a  $1.5 \times 1.2 \mu\text{m}^2$  area on the sample instead of using a fixed focused beam; this, in order to minimize the irradiation dose and the e-beam induced modifications.

The surface morphology of the h-BN exfoliated layers was investigated by atomic force microscopy with a Dimension 3100 Scanning Probe Microscope (Brukers) operating in tapping mode with commercial MPP-11100 probes.

### III. RESULTS AND DISCUSSION

#### A. Luminescence of the bulk material

The h-BN crystallites are often made of a few single crystals separated by grain boundaries, as for another powder studied in a previous work.<sup>13</sup> Thanks to the electron diffraction patterns observed by transmission electron microscopy (TEM) on the specimen presented in Figure 1a, each grain could be precisely orientated along the (00.1) zone axis (not shown here, for experimental details, see Ref.[13]). The TEM experiment shows that the two main grains of the crystallite in Figure 1a are slightly tilted one respect to the other. They are separated by the grain boundary labeled #1.

CL spectra recorded on different areas (labelled #1 and #2) of the crystallite in Figure 1a are shown in Figure 2. They are compared to the one recorded on the HPHT reference sample and called hereafter the reference spectrum. It is worth mentioning that this reference sample

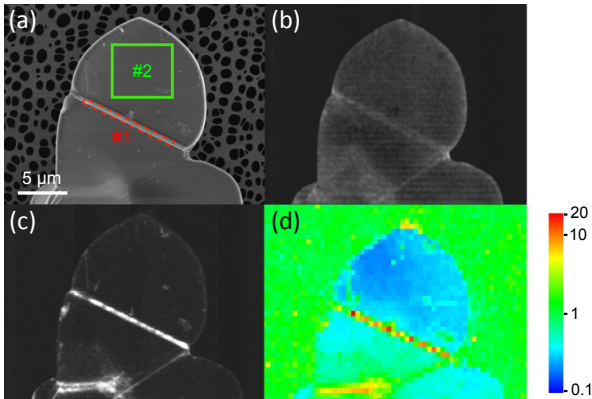


FIG. 1: Images of the bulk material: (a) SEM image of the analyzed crystallite; (b) (c) Corresponding monochromatized CL images recorded at (b) 5.76 eV (215 nm), centered on the main S band emission and at (c) 5.46 eV (227 nm), centered on the main D band emission; (d) D/S ratio between the structural defect-related and the intrinsic excitonic recombinations, extracted from a 64x48 CL hyperspectral-mapping.

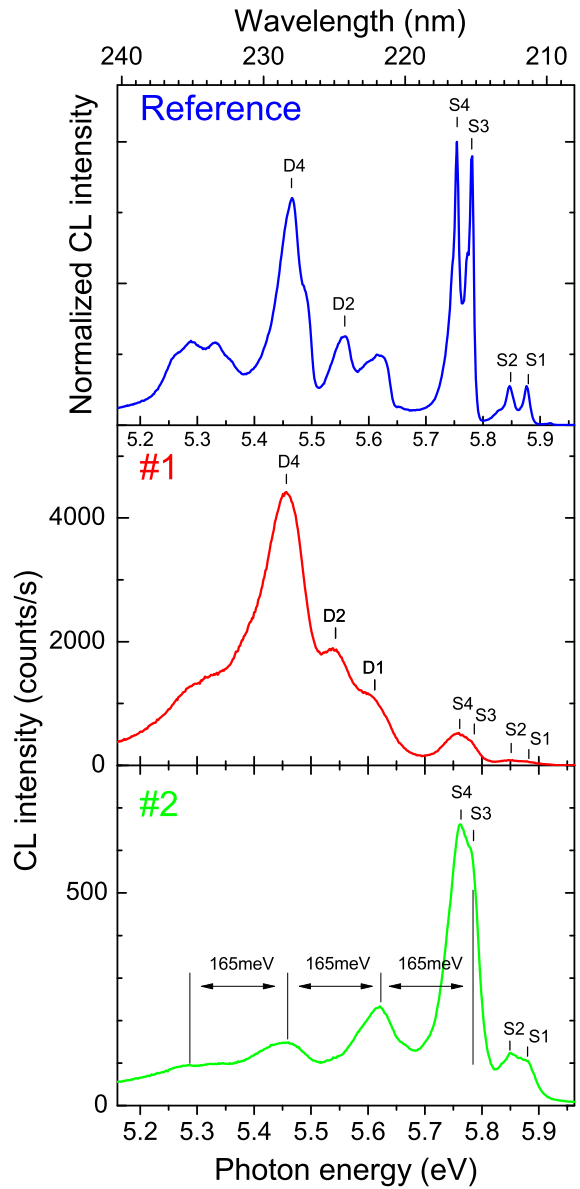


FIG. 2: CL spectra of the bulk h-BN materials in the near-band edge region: at the top is a reference spectrum of a HPHT high quality crystal<sup>28</sup>, compared to #1, registered in the grain boundary area delimited by the red rectangle (averaged over 15 spectra) and to #2 on the main grain of the crystallite in the area delimited by the green square (averaged over 240 spectra), as labeled in Figure 1a. The specimen temperature is about 20 K.

rigorously displays the same S and D lines than the ones observed in the high spectral resolution PL experiments done on a similar single crystal as reported in Ref. [14]. Namely, considering the D band, the maximum of light emission is detected at 5.466 eV, corresponding to the D4 line. The D2 line is seen at 5.557 eV. The broad band centered at 5.61 eV is probably composed of the D1 line

and of the 220 nm band (reported by Watanabe et al.<sup>34</sup>). For the S band, the maximum is observed at 5.754 eV corresponding to the S4 line. A similar feature is observed at 5.780 eV, corresponding to S3 line. Finally two peaks at 5.847 eV and 5.876 eV are observed for respectively S2 and S1 lines.

The spectrum #1 in Figure 2 is recorded at the grain boundary of the h-BN crystallite. It presents the same features as the reference sample, with clear S and D bands. We remark nevertheless that the relative intensities of S and D band are very different. The S band is very weak while the whole spectrum is dominated by the D band. It is known that this latter band is linked to the presence of structural defects as grain boundaries or dislocations.<sup>13,14</sup> To confirm this interpretation, monochromatic images have been registered, at energy centered on the S4 line (at 5.76 eV, Figure 1b) and on the D4 band (at 5.46 eV, Figure 1c). A clear one-to-one correlation is observed between the D series emission and the grain boundary locations (Figure 1a and 1c), while the S series emission appears homogeneous over the crystallite.

To better quantify this view and to dispose of a comparison criterion, we introduce the ratio D/S as the ratio of the intensity of the D band over that of the S band. D/S ratio can be viewed as a measure of the defect density, in the same way than in conventional semiconductors. In this class of materials, the luminescence ratio of bound to free exciton recombinations is an indicator of the crystal purity, being quantitative for indirect bandgap materials such as silicon<sup>35</sup> or diamond.<sup>36</sup> Considering the CL spectral mapping reported in Figure 1d, the D/S ratio is calculated from the CL signals at 5.46 eV and 5.77 eV (resp. 227 and 215 nm). It varies from 0.2 to 20 in the studied h-BN sample. By comparison, in the HPHT sample, the D/S ratio is observed to be highly inhomogeneous from place to place and always higher than 0.8. This means that the single crystal contains a defect density higher than in the core of these grains, which are almost exempt of defects.

Therefore the CL spectrum recorded from the main grain of the crystallite of Figure 1a (spectrum #2 of Figure 2) can be considered as the intrinsic emission of h-BN. Furthermore, because the D band almost vanishes, new features are revealed which were, in previously studied samples, always hindered by the dominant feature of the D band. As a result, three new lines are seen at 5.619, 5.457 and 5.285 eV. Since they are shifted by  $n$  (with  $n = 1, 2, 3$ ) times 165 meV ( $1330 \text{ cm}^{-1}$ ) from the S3-4 band and characterized by a monotonous decay in intensity upon increasing  $n$ , we attribute these lines to three phonon replica of the dominant S lines. The period is close to the 169 meV ( $1363 \text{ cm}^{-1}$ ) optical phonon mode at the center of the Brillouin zone.<sup>37</sup> Phonon replica involving local vibrational modes have already been reported in h-BN for the deep impurity band around 4 eV.<sup>38</sup> They attest of the strong electron-phonon coupling which occurs in this material. Such a coupling is also expected to

have some manifestation on the near-band-edge exciton recombinations. The better quality of some parts of this crystallite and the CL local probe allow us to elucidate this point.

The position in energy of the different bands can also be compared. In the spectrum #1 (at the grain boundary), the D4 and D2 bands are observed respectively at 5.457 eV and 5.537 eV. The S series is detected at 5.756 eV, with a shoulder at 5.78 eV, and with a smaller peak at 5.848 eV with a shoulder at 5.88 eV. The D lines are shifted toward lower energies of about 15 meV when compared to the reference spectrum. Such a decrease of the exciton emission energy could be attributed to a change in the bandgap energy, caused by residual strain differences between the reference HPHT sample and the crystallite. Strain effects are likely to be imputed to the growth method, a phenomenon well known in others standard semiconductors. Since this shift is only observed for the D band, it can also be simply due to a different binding energy of the exciton to the grain boundary. For the spectrum #2, as said previously, only the S band is seen. More precisely, we observe a dominant peak at 5.762 eV with a shoulder at 5.782 eV, and a smaller peak at 5.850 eV with a shoulder at 5.880 eV, attributed to the S4, S3, S2, S1 exciton recombinations, respectively. Compared to the reference spectrum, these bands are broader, despite a higher structural quality. This is mainly due to the fact that it is an averaged spectrum, and very small changes are observed in the exciton emission energy at different positions on the grain. Nevertheless this energy difference, and also with the spectrum #1 and the reference spectrum, is of only few meV, much less than the differences seen on the D band.

## B. Thickness of the exfoliated layers

Turning now to the exfoliated sheets from this powder, several sheets have been studied from which we show three representative samples in Figure 3. The surface of each h-BN flake was scanned by AFM in tapping mode in order to measure their thickness, consecutively to the CL studies. The sheet surface is not completely flat, some prominent dots being visible. Most probably they are adhesive tape glue residues from the exfoliation process. Some small 10-100 nm size holes are also observable. It is not clear whether they were already in the bulk material or whether they are due to electron exposure as reported in the literature. Indeed etching under electron beam in a transmission electron microscope, even at low acceleration voltage, cannot be avoided.<sup>39-42</sup> Aside from this, the flakes appear to be well spread on top of the  $\text{SiO}_2$  substrate.

Particular attention has been paid to the h-BN layer thickness determination because of the water layer trapped beneath it. This problem is well known in the case of graphene on  $\text{SiO}_2$ <sup>32,33</sup> and already mentioned for h-BN on  $\text{SiO}_2$ .<sup>30</sup> This property of graphene has even been

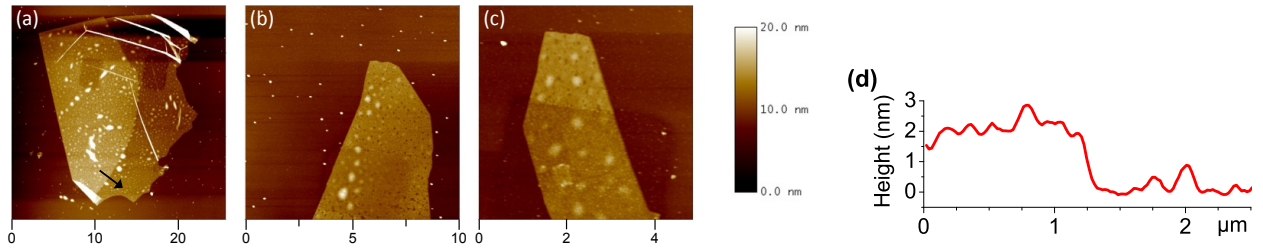


FIG. 3: AFM images of exfoliated h-BN layers transferred onto a SiO<sub>2</sub>/Si substrate: (a) sample A; (b) sample B; (c) sample C. The image size unit is the micrometer. (d) Profile taken across the fold back part of the sheet A, along the arrow shown in (a).

	Sample A	Sample B	Sample C
Average thickness (nm)	$2.1 \pm 0.1$ (5)	$2.8 \pm 0.6$ (5)	$3.4 \pm 0.4$ (4)
Number of atomic layers	$6 \pm 1$	$8 \pm 2$	$10 \pm 2$

TABLE I: Summary of AFM thickness measurements on exfoliated h-BN layers shown in Figure 3. The number of measurements over which the average and the standard deviation are calculated is indicated in parenthesis.

used recently to build membranes keeping water under the liquid phase for TEM observation under vacuum.<sup>43</sup>

Due to the presence of the water layer, the height profiles taken on steps by AFM at the flake edges overestimate the h-BN thickness. The special geometry of sample A, which displays a part fold back on itself, gives the key to solve this problem. The step height of the fold part gives a thickness measurement independent of the amount of water trapped between h-BN and SiO<sub>2</sub>, and this measurement has been used as the reference for the thickness measurement as follows. The h-BN flake thickness is found to be equal to a value of 2.1 nm averaged over nine step height measurements along the edge (see Figure 3d). The standard deviation is found below 0.33 nm, the interplanar distance along the *c* axis in h-BN. This shows that the thickness of flake A is homogeneous. Still considering the h-BN interplanar distance, the exfoliated sample A is about six atomic layers thick. Then the water layer thickness is deduced by difference with the step edges and is found equal to  $1.9 \text{ nm} \pm 0.25 \text{ nm}$  over seven measurements. The thicknesses of sample B and C are measured assuming a homogenous water layer thickness over the wafer. The results are summarized in Table I.

One can notice that the areas scanned during the CL acquisition appear as dark rectangles in AFM images, which indicates a lower height. This could be interpreted by an electron beam induced etching. As we can also observe a lower height on the SiO<sub>2</sub>, it is more probably a reduction of the volume of the amorphous silica under irradiation.<sup>44</sup> Nevertheless, as we already mentioned, BN materials etching under electron beam cannot be excluded.<sup>39-42</sup> Moreover ice under the flake could help this etching by a chemical effect, as it has been reported in the case of graphene.<sup>45</sup> Indeed an evolution of the luminescence spectra under exposure is observed, indicating that the BN structure could have been modified.

### C. Excitonic recombinations in h-BN exfoliated layers

The CL spectra of the three exfoliated h-BN layers presented above are shown in Figure 4. First of all, as expected, the CL intensity decreases when decreasing the h-BN layer thickness. This is understandable as a nanometer-thick h-BN layer is transparent to the electron beam, so that the electron-hole generation in such a thin layer is directly proportional to its thickness. Excitonic recombinations of exfoliated layers are systematically dominated by the D series. This is somewhat surprising since we have shown that the intrinsic S emissions dominate CL spectra outside grain boundaries. This could indicate a higher concentration of structural defects in the exfoliated samples. Several phenomena could be responsible for this defect creation in the exfoliated layers: (i) a water layer freezing at the low temperature used for CL experiments and the resulting induced deformation (ii) damages induced by the exfoliation process itself or (iii) defect generation induced by electron beam irradiation at low temperature. At the present time, it appears difficult to discriminate between them.

Compared to the h-BN reference spectrum from the HPHT crystal, the spectra of exfoliated layers present exactly the same D4 and D2 lines related to the D band, and unresolved S3-S4 and S1-S2 lines related to the S band. Looking in more detail at the D series emission, we observe a shift from 5.471 eV for the bulk to 5.477, 5.479 and 5.499 eV for exfoliated samples C (10 ML), B (8 ML) and A (6 ML) respectively. The shift of the intrinsic S line emissions is hard to define because of a low signal to noise ratio. As already discussed previously, shift in energy of the emission lines compared to the reference spectrum is caused by strain variations. Here we have to explain why, while the h-BN layer thickness decreases

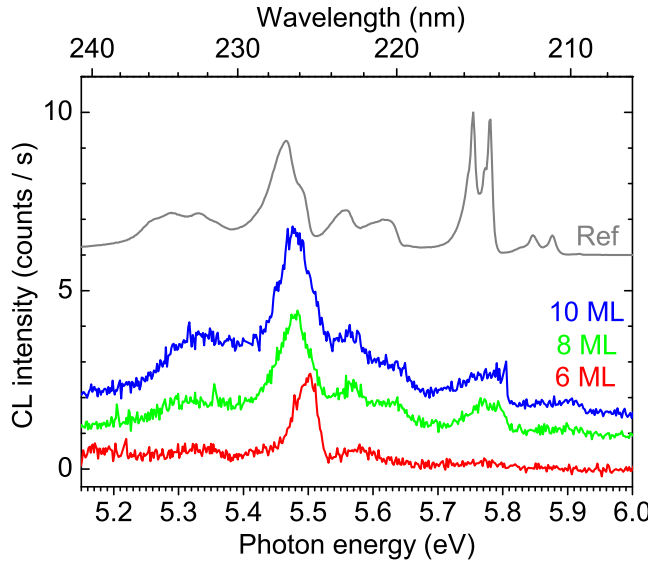


FIG. 4: Near-band-edge exciton recombinations from exfoliated h-BN layer A (6 ML), B (8 ML) and C (10 ML) compared to the normalized reference spectrum (from HPHT crystal). The zero of CL spectra was shifted for clarity.

from 10 to 6 ML, the emission is shifting toward higher energies.

This shift can be understood as follows. Since in h-BN, the exciton is theoretically expected to be mostly localized within one layer, a quantum confinement can affect the optical response for a large reduction in thickness only. Screening becomes then less efficient and the exciton binding energy is expected to increase. Theoretical calculations by Wirtz et al.<sup>46</sup> show that the situation is slightly more complex. In these calculations, the optical response of a single sheet of h-BN is considered as a function of the intersheet distance in a supercell geometry. The result is that indeed the exciton binding energy increases when this distance increases, but that simultaneously the quasiparticle band gap calculated within the GW approximation increases, so that the net result is a weak blue shift, about 200 meV, in the error bar of such calculations. Similar effects are observed in the case of BN nanotubes when their diameter decreases,<sup>46,47</sup> and more recently in nanoribbons.<sup>48</sup> Although no calculation has been performed explicitly concerning the effect of the number of layers, the above arguments indicate that the effect is expected to be weak down to a few layers and should not exceed a few tenths of eV anyway. This is in agreement with our results, which show a small increase (20 meV) in the exciton recombination energy for a 6 ML sheet. Further calculations as well as experiments for less than five layers would be of great interest to see if larger effects are then observed.

More generally, this work reports luminescence spectra of a semiconductor only a few atomic layers thick, which is not common. Indeed in nanostructures, the lumines-

cence is often quenched at very low size, due to dominating surface effects, since extremely large surface to volume ratio is present in nanomaterials such as nanowires or colloidal quantum dots. Surface band-bending and as well non radiative surface recombinations are often responsible for the absence of luminescence in these materials in the nanometer range.<sup>49,50</sup> The presence of dangling bonds or adsorbed atoms could also change the optical response of the nanomaterial. The control of the surface by its passivation is thus the subject of intense research. This is often achieved by growing a shell made of a higher band gap material. This results in a dramatic enhancement of the quantum efficiency, sometimes of several order of magnitude.<sup>51–54</sup> In few layers BN our results indicate that such a passivation is not necessary. The layered nature of h-BN with a  $sp^2$ -bonding combined with the strong localization of the exciton at the atomic layer scale could prevent surface effects. This can be of great interest for future optical applications and devices.

#### IV. CONCLUSION

In conclusion, we have studied high quality crystallites by cathodoluminescence and compared them with exfoliated sheets in the near-band edge region of h-BN, around 5.5 eV. Two main results have been obtained. First thanks to the high quality of the crystallites, we could, for the first time, clearly discriminate the luminescence of structure defects free areas (dominated by the S band) and that of defected zones (dominated by the D band). In defected zones such as grain boundaries, excitons are bounded to the defects, resulting in a red-shift of their emission energy. From this, we propose a simple and workable parameter for evaluating the structure defect density in h-BN samples, using their near-band-edge emission. This parameter is defined as the ratio of the intensity of the D band over that of the S band. Furthermore, the observation of defect free areas has revealed new features, attributed to phonon replica of the excitons. Secondly, investigation of the emission of exfoliated sheets has shown that the reduction in thickness induces a slight increase of the bound-exciton emission energy. Although confinement effects are expected to occur in very thin layers, one cannot exclude detrimental effects, such as roughness and surface charges of the  $SiO_2$  substrate used for supporting exfoliated sheets. Further experiments on free-standing sheets are thus in progress, with the advantage to make possible correlations between the emission and structural features thanks to TEM observations.

#### ACKNOWLEDGMENTS

T. Taniguchi and K. Watanabe from NIMS, Japan, are warmly acknowledged for providing one of their HPHT crystals. The authors would like to thank S. Pouget

from CEA Grenoble for X-ray experiments, C.Vilar from GEMaC for her technical help on the cathodoluminescence SEM set-up, and H. Mariette from NPSC for fruitful discussions. This work has been supported by the

CNRS Mission Interdisciplinaire (“Graphene” Challenge of the G3N program) and by the ONERA “Graphene” Federative Research Program. A. P. thanks C’Nano Rhône Alpes and Ile-de-France for financial support.

---

<sup>\*</sup> Current address: Hitachi Cambridge Laboratory, J. J. Thomson Avenue, Cambridge CB23 7GP, United Kingdom

<sup>1</sup> Chopra N G, Luyken R J, Cherrey K, Crespi V H, Cohen M L, Louie S G and Zettl A 1995 *Science* **269** 966

<sup>2</sup> Loiseau A, Willaime F, Demoncey N, Hug G and Pascard H 1996 *Phys. Rev. Lett.* **76** 4737

<sup>3</sup> Shi Y, Hamsen C, Jia X, Kim K K, Reina A, Hofmann M, Hsu A L, Zhang K, Li H, Juang Z Y, Dresselhaus M S, Li L J and Kong J 2010 *Nano Lett.* **10** 4134

<sup>4</sup> Song L, Ci L, Lu H, Sorokin P, Jin C, Ni J, Kvashnin A, Kvashnin D, Lou J, Yakobson B and Ajayan P M 2010 *Nano Lett.* **10** 3209

<sup>5</sup> Zunger A, Katzir A and Halperin A 1976 *Phys. Rev. B* **13** 5560

<sup>6</sup> Museur L, Brasse G, Pierret A, Maine S, Attal-Tretout B, Ducastelle F, Loiseau A, Barjon J, Watanabe K, Taniguchi T and Kanaev A 2011 *Phys. Status Solidi RRL* **5** 214

<sup>7</sup> Blase X, Rubio A, Louie S G and Cohen M L 1995 *Phys. Rev. B* **51** 6868

<sup>8</sup> Dean C, Young A, Meric I, Lee C, Wang L, Sorgenfrei S, Watanabe K, Taniguchi T, Kim P, Shepard K and Hone J 2010 *Nat. Nanotechnol.* **5** 722

<sup>9</sup> Xue J, Sanchez-Yamagishi J, Bulmash D, Jacquod P, Deshpande A, Watanabe K, Taniguchi T, Jarillo-Herrero P and LeRoy B 2011 *Nat. Mater.* **10** 282

<sup>10</sup> Gannett W, Regan W, Watanabe K, Taniguchi T, Crommie M F and Zettl A 2011 *Appl. Phys. Lett.* **98** 242105

<sup>11</sup> Decker R, Wang Y, Brar V W, Regan W, Tsai H Z, Wu Q, Gannett W, Zettl A and Crommie M F 2011 *Nano Lett.* **11** 2291

<sup>12</sup> Britnell L, Gorbachev R V, Jalil R, Belle B D, Schedin F, Mishchenko A, Georgiou T, Katsnelson M I, Eaves L, Morozov S V, Peres N M R, Leist J, Geim A K, Novoselov K S and Ponomarenko L A 2012 *Science* **335** 947–950

<sup>13</sup> Jaffrennou P, Barjon J, Lauret J S, Attal-Trétout B, Ducastelle F and Loiseau A 2007 *J. Appl. Phys.* **102** 116102

<sup>14</sup> Watanabe K and Taniguchi T 2009 *Phys. Rev. B* **79** 193104

<sup>15</sup> Museur L and Kanaev A 2008 *J. Appl. Phys.* **103** 103520

<sup>16</sup> Wirtz L, Marini A, Grüning M and Rubio A 2005 *ArXiv:cond-mat/0508421*

<sup>17</sup> Arnaud B, Lebègue S, Rabiller P and Alouani M 2006 *Phys. Rev. Lett.* **96** 026402

<sup>18</sup> Wirtz L, Marini A, Grüning M, Attaccalite C, Kresse G and Rubio A 2008 *Phys. Rev. Lett.* **100** 189701

<sup>19</sup> Arnaud B, Lebègue S, Rabiller P and Alouani M 2008 *Phys. Rev. Lett.* **100** 189702

<sup>20</sup> Kim K K, Hsu A, Jia X, Kim S M, Shi Y, Hofmann M, Nezich D, Rodriguez-Nieva J F, Dresselhaus M, Palacios T and Kong J 2012 *Nano Lett.* **12** 161

<sup>21</sup> Wang X, Pakdel A, Zhi C, Watanabe K, Sekiguchi T, Golberg D and Bando Y 2012 *J. Phys.: Condens. Matter* **24** 314205

<sup>22</sup> Ismach A, Chou H, Ferrer D A, Wu Y, McDonnell S, Floresca H C, Covacevich A, Pope C, Piner R, Kim M J, Wallace R M, Colombo L and Ruoff R S 2012 *ACS Nano* **6** 6378

<sup>23</sup> Pakdel A, Wang X, Zhi C, Bando Y, Watanabe K, Sekiguchi T, Nakayama T and Golberg D 2012 *J. Mater. Chem.* **22**(11) 4818

<sup>24</sup> Ci L, Song L, Jin C, Jariwala D, Wu D, Li Y, Srivastava A, Wang Z, Storr K, Balicas L, Lui F and Ajayan P M 2010 *Nat. Mater.* **9** 430

<sup>25</sup> Lin Y, Williams T and Connell J 2009 *The J. Phys. Chem. Lett.* **1** 277

<sup>26</sup> Gao G, Gao W, Cannuccia E, Taha-Tijerina J, Balicas L, Mathkar A, Narayanan T N, Liu Z, Gupta B K, Peng J, Yin Y, Rubio A and Ajayan P M 2012 *Nano Letters* **12** 3518

<sup>27</sup> Li L H, Chen Y, Cheng B M, Lin M Y, Chou S L and Peng Y C 2012 *Appl. Phys. Lett.* **100** 261108

<sup>28</sup> Taniguchi T and Watanabe K 2007 *J. Cryst. Growth* **303** 525

<sup>29</sup> Novoselov K, Geim A, Morozov S, Jiang D, Zhang Y, Dubonos S, Grigorieva I and Firsov A 2004 *Science* **306** 666

<sup>30</sup> Gorbachev R V, Riaz I, Nair R R, Jalil R, Britnell L, Belle B D, Hill E W, Novoselov K S, Watanabe K, Taniguchi T, Geim A K and Blake P 2011 *Small* **7** 465

<sup>31</sup> Betz A 2012 *RF dynamics and noise of graphene microwave devices* Ph.D. thesis Paris VI University

<sup>32</sup> Nagashio K, Yamashita T, Nishimura T, Kita K and Toriumi A 2011 *J. Appl. Phys.* **110** 024513

<sup>33</sup> Ishigami M, Chen J H, Cullen W G, Fuhrer M S and Williams E D 2007 *Nano Letters* **7** 1643

<sup>34</sup> Watanabe K, Taniguchi T, Miya K, Sato Y, Nakamura K, Niiyama T and Taniguchi M 2011 *Diamond Relat. Mater.* **20** 849

<sup>35</sup> Broussell I, Stotz J A H and Thewalt M L W 2002 *J. Appl. Phys.* **92** 5913

<sup>36</sup> Barjon J, Tillocher T, Habka N, Brinza O, Achard J, Issaoui R, Silva F, Mer C and Bergonzo P 2011 *Phys. Rev. B* **83**(7) 073201

<sup>37</sup> Serrano J, Bosak A, Arenal R, Krisch M, Watanabe K, Taniguchi T, Kanda H, Rubio A and Wirtz L 2007 *Phys. Rev. Lett.* **98** 095503

<sup>38</sup> Silly M G, Jaffrennou P, Barjon J, Lauret J S, Ducastelle F, Loiseau A, Obraztsova E, Attal-Trétout B and Rosencher E 2007 *Phys. Rev. B* **75** 085205

<sup>39</sup> Jin C, Lin F, Suenaga K and Iijima S 2009 *Phys. Rev. Lett.* **102** 195505

<sup>40</sup> Suenaga K, Kobayashi H and Koshino M 2012 *Phys. Rev. Lett.* **108**(7) 075501

<sup>41</sup> Alem N, Ramasse Q M, Seabourne C R, Yazyev O V, Erickson K, Sarahan M C, Kisielowski C, Scott A J, Louie S G and Zettl A 2012 *Phys. Rev. Lett.* **109**(20) 205502

<sup>42</sup> Pan C T, Nair R R, Bangert U, Ramasse Q, Jalil R, Zan R, Seabourne C R and Scott A J 2012 *Phys. Rev. B* **85**(4) 045440

<sup>43</sup> Yuk J M, Park J, Ercius P, Kim K, Hellebusch D J, Crommie M F, Lee J Y, Zettl A and Alivisatos A P 2012 *Science* **336** 61

<sup>44</sup> Kalceff M A S, Phillips M R and Moon A R 1996 *J. Appl. Phys.* **80** 4308

<sup>45</sup> Gardener J A and Golovchenko J A 2012 *Nanotechnology* **23** 185302

<sup>46</sup> Wirtz L, Marini A and Rubio A 2006 *Phys. Rev. Lett.* **96** 126104

<sup>47</sup> Park C H, Spataru C D and Louie S G 2006 *Phys. Rev. Lett.* **96** 126105

<sup>48</sup> Wang S, Chen Q and Wang J 2011 *Appl. Phys. Lett.* **99** 063114

<sup>49</sup> Demichel O, Heiss M, Bleuse J, Mariette H and Fontcuberta i Morral A 2010 *Appl. Phys. Lett.* **97** 201907

<sup>50</sup> Calarco R, Stoica T, Brandt O and Geelhaar L 2011 *J. Mater. Res.* **26** 2157

<sup>51</sup> Hines M A and Guyot-Sionnest P 1996 *J. Phys. Chem.* **100** 468

<sup>52</sup> Peng X, Schlamp M C, Kadavanich A V and Alivisatos A P 1997 *J. Am. Chem. Soc.* **119** 7019

<sup>53</sup> Couto O D D, Sercombe D, Puebla J, Otubo L, Luxmoore I J, Sich M, Elliott T J, Chekhovich E A, Wilson L R, Skolnick M S, Liu H Y and Tartakovskii A I 2012 *Nano Lett.* **12** 5269

<sup>54</sup> Titova L V, Hoang T B, Jackson H E, Smith L M, Yarrison-Rice J M, Kim Y, Joyce H J, Tan H H and Jagadish C 2006 *Appl. Phys. Lett.* **89** 173126